Available online at www.sciencedirect.com
SCIENCE DIRECT®

Organic Geochemistry 37 (2006) 189–207

Organic Geochemistry

www.elsevier.com/locate/orggeochem

Contrasting sterane signatures in Neoproterozoic marine rocks of Australia before and after the Acraman asteroid impact

David M. McKirdy [a,*], Lynn J. Webster [a], Khaled R. Arouri [a,1], Kathleen Grey [b], Victor A. Gostin [a]

[a] Organic Geochemistry in Basin Analysis Group, School of Earth and Environmental Sciences, University of Adelaide, SA 5005, Australia
[b] Geological Survey of Western Australia, Department of Industry and Resources, 100 Plain Street, East Perth, WA 6004, Australia

Received 2 March 2005; accepted 21 September 2005
(returned to author for revision 9 May 2005)
Available online 5 December 2005

Abstract

Organic matter preserved in marine mudstones from three late Neoproterozoic depocentres – the Officer and Amadeus Basins and the Adelaide Fold Belt – was examined using standard microscopic and geochemical methods, including gas chromatography-mass spectrometry (GC–MS). Total organic carbon (TOC) contents of these sediments are typically low (<0.25%) and the thermal maturity (expressed as calculated vitrinite reflectance, Rc, based on measured methylphenanthrene index) is in the range 0.68–1.35%. Samples of drill core spanned the interval containing ejecta from the impact of a large chondritic asteroid at ca. 570 Ma. The remnant structure caused by the impact is located at Lake Acraman on the Gawler Craton. Palynological studies reveal a major change from the impoverished microbial and leiosphere palynoflora that survived the postulated "Snowball Earth" glaciation of Marinoan age (ca. 580 Ma) to one dominated by large complex acritarchs (acanthomorphs) following the Acraman impact. Among the benthic and planktonic inputs to these sediments, the eukaryotic steroidal biomarkers provide clear evidence of the environmental havoc wrought by the impact. C_{29}/C_{27} sterane ratios increase from 0.7–1.3 below the ejecta horizon to 1–11 above it. This suggests that primitive cyst-forming chlorophytes with a robust reproductive cycle survived in the immediate aftermath of the impact, whereas other algae (including the leiospheroid prasinophytes) were less resilient. A corresponding fourfold drop in sterane/hopane ratios is consistent with a negative shift of 4‰ in $\delta^{13}C_{org}$ at about this time, both signalling a sharp decline in marine algal productivity. On the basis of evidence from Australia and Oman, the estimated duration of this anomalous marine sterane signature is at least 20 million years. It corresponds to the opportunistic proliferation of new chlorophyte taxa in the aftermath of the Acraman event.

1. Introduction

For the most part, bolide impacts appear to have been of remarkably little interest to organic geochemists. This is surprising, given that large asteroidal or cometary impacts are likely to have had a

* Corresponding author. Tel.: +61 8 8303 5378; fax: +61 8 8303 4347.
E-mail address: david.mckirdy@adelaide.edu.au (D.M. McKirdy).
1 Present address: R&D Center, Saudi Aramco, P.O. Box 1528, Dhahran 31311, Saudi Arabia.

0146-6380/$ - see front matter.
doi:10.1016/j.orggeochem.2005.09.005

drastic effect on the abundance and diversity of marine and terrigenous biota because of, inter alia, loss of sunlight, increased water turbidity, forest fires, acid rain and global cooling (Kring, 2000). Although there is now less enthusiasm for equating Phanerozoic extinction events with impacts, several of the more notable mass extinctions in Earth history were attributed by Raup (1992) to catastrophic bolide impacts that left craters >50 km in diameter. Pre-eminent among these is the 180-km diameter Chicxulub crater on the Yucatan Peninsula and its link to the well-documented Cretaceous/Tertiary (K-T) extinction that wiped out 75% of extant species 65 Ma. Another is the impact that produced the 52-km Siljan Crater in Sweden and which may have led to the less severe Frasnian-Fammenian marine extinction at 368 Ma. Such extinctions typically involve major restructuring of oceanic water circulation patterns, as well as fundamental changes in marine microfossil assemblages (see, e.g., Poag, 1997; Coccioni et al., 2000).

Both the above impacts were the subjects of at least preliminary organic geochemical studies. Charcoal, soot ($\delta^{13}C = -25.8 \pm 0.6‰$), retene and other PAHs produced by the burninig of terrigenous vegetation in post-impact wildfires are widespread in the K-T boundary layer (Venkatesan and Dahl, 1989; Wolbach et al., 1990; Ivaney and Salawitch, 1993), along with fullerenes of possible extraterrestrial origin (Heymann et al., 1994; Becker et al., 2000). Heating by the Siljan impact generated 'instant' crude oil from local Ordovician shales that hitherto were thermally immature (Vlierboom et al., 1986). More recently, Becker et al. (2001) discovered noble gas-bearing fullerenes (C_{60} to C_{200}) in sediments from the Permo-Triassic boundary in China and Japan, corresponding to the largest mass extinction in the Phanerozoic record, and attributed them to a yet-to-be-confirmed bolide impact. However, the latter inference is not supported by the recent findings of Grice et al. (2005) who identified widespread photic zone euxinia as a driver of this extinction. Extinction events commonly are marked by sharp negative excursions of 1–3‰ in the pelagic-to-benthic $\delta^{13}C_{carb}$ gradient (Hsü and McKenzie, 1990; Holser, 1997; and references therein), signalling a collapse of marine primary productivity under the global dust cloud thrown up by the impact. The secular $\delta^{13}C_{org}$ profile (McLaren and Goodfellow, 1990) of an extinction may be complicated or obscured by changes in organic facies (e.g., Foster et al., 1997). As yet, however, there has been no concerted attempt to search the marine sedimentary record for molecular biomarker signals of such environmental disasters. The present study focusses on one of Australia's oldest and largest impact craters, located at Lake Acraman on the Eyre Peninsula of South Australia (Fig. 1; Gostin et al., 1986; Williams, 1986, 1994).

2. Sedimentology and age of Acraman impact ejecta layer and its host formation

Investigations of the Acraman crater and the sedimentology and geochemistry of its associated ejecta have generated extensive literature, recently summarised by Williams and Wallace (2003). The deeply eroded remnant crater occurs in the Gawler Range Volcanics, a suite of Mesoproterozoic continental lavas and ash flows. It was produced by the impact of a large chondritic asteroid on the Gawler Craton at Lake Acraman (latitude 32°01′S, longitude 135°26′E). Although the age of the Acraman event is not well constrained (see below) the presence of the ejecta layer in the Bunyeroo Formation of the Adelaide Fold Belt (Gostin et al., 1986, 1989; Wallace et al., 1989, 1996; Williams, 1986, 1994; Williams et al., 2004; Williams and Wallace, 2003)

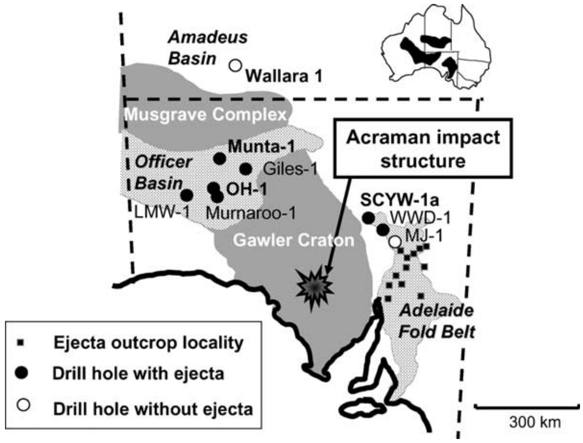

Fig. 1. Location of the Acraman impact structure on the Gawler Craton and of the adjacent Officer Basin, Amadeus Basin and Adelaide Fold Belt. The dark areas on the map of mainland Australia (inset) indicate the full extent of the three Ediacaran depocentres. The four drill holes highlighted in bold font are those from which core was sampled for analysis. In the Observatory Hill-1 well the ejecta layer is present at 355.0 m; in the Munta-1 well ejecta occurs as reworked rock fragments, whereas that identified in SCYW-1a comprises only fractured zircons and other acid-insoluble non-silicate crystals in palynological residues. Based on information from Wallace et al. (1996) and Hill et al. (2004).

shows that it lies well above the base of the Ediacaran System. The Global Stratotype and Section Point marking the base of the Ediacaran was recently ratified as being at the base of the Nuccaleena Formation, the 'cap dolomite' above the Elatina Formation, better known as the Marinoan glaciation (Knoll et al., 2004).

The target rock was the Yardea Dacite, fragments of which are readily identified in the ejecta layer within the adjacent marine depocentres of the Adelaide Fold Belt to the east and the Officer Basin to the northwest (Fig. 1). The physical characteristics of the impact are outlined in Table 1. Its impact energy exceeded the nominal threshold for global catastrophe (Toon et al., 1997) and the likely effects included earthquakes, tsunami, injection of stratospheric water vapour, ozone loss and the dispersal of a global dust cloud. Light levels would have dropped below those that can support photosynthesis. An impact of this size during the Phanerozoic would have scored a 47% kill rate on Raup's (1992) extinction curve for marine species. The dust cloud associated with the impact is likely to have been considerably larger than one generated in the Phanerozoic because the land surface was not vegetated and would have lacked well developed humic-rich soils. The land surface probably bore a closer resemblance to present day lunar or Martian surfaces and a substantial amount of fine dust could be expected to be mobilized by the blast fronts associated with the bolide impact. Palaeomagnetic studies place the Acraman locality at 12.5°N at the time of the impact (Williams and Wallace, 2003; Williams et al., 2004). This low palaeolatitude is crucial because it permitted the ensuing atmospheric dust cloud to affect both hemispheres. Thus, the age (pre-Devonian), magnitude and location of the Acraman impact conspired to wreak global environmental havoc.

The timing of the impact is recorded by an ejecta layer in the deep water marine shales of the Bunyeroo Formation in the Adelaide Fold Belt (Gostin et al., 1986; Wallace et al., 1996) to the east of the impact site (Fig. 1). A similar but somewhat thinner layer of finer-grained ejecta detritus occurs low in the Dey Dey Mudstone of the Eastern Officer Basin, some 500 km to the northwest (Wallace et al., 1989). Preiss (2000) considered a Rb–Sr whole rock isochron of 588 ± 35 Ma from the Yarloo Shale, a Bunyeroo Formation equivalent in drill-hole SCYW-1a on the Stuart Shelf (Fig. 1), to be one of the more reliable dates on the stratigraphic interval hosting the ejecta layer. Walter et al. (2000) suggested a best estimate of 578 Ma for the timing of the impact event by interpolation of probable ages between established dates, but this involved correlating the glaciomarine Elatina Formation with the approximately 605 Ma Icebrook Formation, a diamictite in northwest Canada. Recent dating by Calver et al. (2004) of rhyodacite underlying the Croles Hill diamictite in northern Tasmania and a mafic dyke intruding the correlative Cottons Breccia, another diamictite on nearby King Island, suggests an age between 582 ± 4 Ma and 575 ± 3 Ma for these glacial successions. This dating implies an age of ca. 580 Ma for the Tasmanian glaciation which, when viewed in its stratigraphic context and taking into account $^{87}Sr/^{86}Sr$ ratios in the overlying Smithton Dolomite (Calver, 1998; Calver and Walter, 2000), may reasonably be correlated with the Elatina Formation. This in turn makes the latter essentially the same age as the Gaskiers Tillite of Newfoundland (580 Ma: Bowring et al., 2003). Two other "Marinoan-type" glacial deposits, the Nantuo Tillite in south China (minimum age 599 ± 4 Ma, maximum age 663 ± 4 Ma: Zhou et al., 2004) and the Ghaub Formation in Namibia (635.5 ± 1.2 Ma: Hoffmann et al., 2004), appear to represent another temporally discrete glacial episode. Alternatively, using carbon isotope chemostratigraphy, Halverson et al. (2005) choose to correlate the Elatina Formation with these older glacial successions.

Whatever the precise age of the Marinoan glaciation, the ejecta layer lies some considerable distance above it. In the Stuart Shelf area, the ejecta layer occurs at least 700 m above the Marinoan cap dolomite and, taking into account the relatively slow sedimentation rates and the fact that the impact event took place during the second marine transgression after the glaciation, the ejecta layer is probably about 10 million years younger than the glaciation. It is considerably older than the bilaterian Ediacara fauna, which first appears several hundred metres above the ejecta layer and which,

Table 1
Physical parameters of the Acraman asteroid impact (Williams, 1994; Williams and Wallace, 2003)

Bolide diameter	~4.8 km
Transient cavity	~40 km
Collapse crater	85–90 km
Ejecta blanket radius	>540 km
Estimated energy	5.2×10^6 Mt

from U–Pb zircon dating on a volcanic ash bed in the White Sea region of Russia, is older than 553 ± 0.3 Ma (Martin et al., 1999). This age is broadly consistent with a (probably detrital) zircon grain dated at 556 ± 24 Ma that is present at the base of the Pound Subgroup (Preiss, 2000). Given the available constraints and considering the relative thickness of sediments above and below the ejecta layer, an age between 570 and 580 Ma seems reasonable for the Acraman event.

The lower parts of both units in which the ejecta layer is located also contain ice-rafted sediment and evidence of seasonal 'refrigeration' (dropstones in the Bunyeroo Formation: Jenkins et al., 1998; till pellets and graded bedding in the Dey Dey Mudstone: Webster, 2001; Webster et al., 2004). These sedimentological features are important because they indicate that the near-equatorial Palaeo-Pacific Ocean (Li and Powell, 2001) may have still been subject to glacial influence immediately prior to the impact event. Although less severe than the main Marinoan 'snowball' event, this may have placed further stress on an already decimated marine biota. The Acraman asteroid impact delivered another blow.

Compelling evidence for the dramatic effect of the Acraman impact on the late Neoproterozoic (Ediacaran) biosphere has emerged from recent palynological and carbon isotopic examination of well-preserved marine sediments from three nearby basins (Fig. 1). The microfossil record reveals a sudden change from the impoverished microbial and leiosphere palynoflora that survived the postulated Marinoan "Snowball Earth" glaciation (for the purposes of this paper taken to be ca. 580 Ma: Calver et al., 2004) to one dominated by large complex acritarchs (acanthomorphs) immediately following the Acraman impact (Grey, 2001, 2005; Grey et al., 2003). Coincident with this rapid transition from a simple Ediacaran leiosphere palynoflora (ELP) to the Ediacaran complex acritarch palynoflora (ECAP) is a 4‰ negative excursion in the $\delta^{13}C_{carb}$ and $\delta^{13}C_{org}$ records (Calver, 2000; Calver and Lindsay, 1998). This can reasonably be attributed to a rapid decline in marine biomass and productivity (Margaritz, 1989), although other forcing factors such as decreased burial of organic matter (Holser, 1997) may also have contributed. Another intriguing coincidence is the extremely poor preservation of organic walled microfossils over this transitional interval, in the immediate aftermath of the impact event (Grey et al., 2003).

We report here the first results of an organic geochemical reconnaissance aimed at searching the same Ediacaran succession for biomarker (molecular fossil) evidence of the aforementioned palynofloral and isotopic changes. As molecular chemostratigraphers, we seek to address part of the challenge originally issued by McLaren and Goodfellow (1990): to find a signal of the biological and chemical events associated with the Acraman asteroid impact.

3. Samples and methods

3.1. Sampling strategy

The samples ($n = 49$) comprise drill core from the lower Pertatataka Formation of the Amadeus Basin in the Wallara-1 well and from the Dey Dey Mudstone and overlying Karlaya Limestone (partial correlatives of the upper Pertatataka) of the Officer Basin in the Munta-1 and Observatory Hill-1 wells (Fig. 2). These units were deposited in hemipelagic, turbiditic and marine shelf depositional environments adjacent to the Gawler Craton immediately before, during and after the Acraman event. Their suitability for biomarker analysis is highlighted by several recent studies. Logan et al. (1997) provided biomarker and isotope data on selected samples (TOC = 0.07–0.95 wt%) from these formations. Well-preserved microbial mats and their molecular fossils were described from low in the Pertatataka Formation at the Wallara-1 locality (Logan et al., 1999) and from the Tanana Formation higher in the Neoproterozoic succession penetrated by the Munta-1 well (Arouri et al., 2000a,b). Core samples of the Yarloo Shale (a Bunyeroo equivalent) and shale within the upper ABC Range Quartzite at mineral exploration drill-hole SCYW-1a (Fig. 1) extended coverage of the pre-Acraman time interval.

Sampling for the present study (Table 2, Fig. 2) both overlaps and fills the gaps in the stratigraphic coverage of the previous workers, thereby spanning the Acraman ejecta horizon in the Officer Basin (Wallace et al., 1989; Hill et al., 2004). Although the ejecta layer is not present in the Amadeus Basin, the most distant of the three Ediacaran depocentres (>700 km from the impact site), its level in the succession can be inferred from the local $\delta^{13}C_{org}$ (Calver, 2000) and microfossil (Grey, 2001, 2005) records. The equivalent sediments in the depocentre closest to the impact site (Adelaide Fold Belt; Fig. 1)

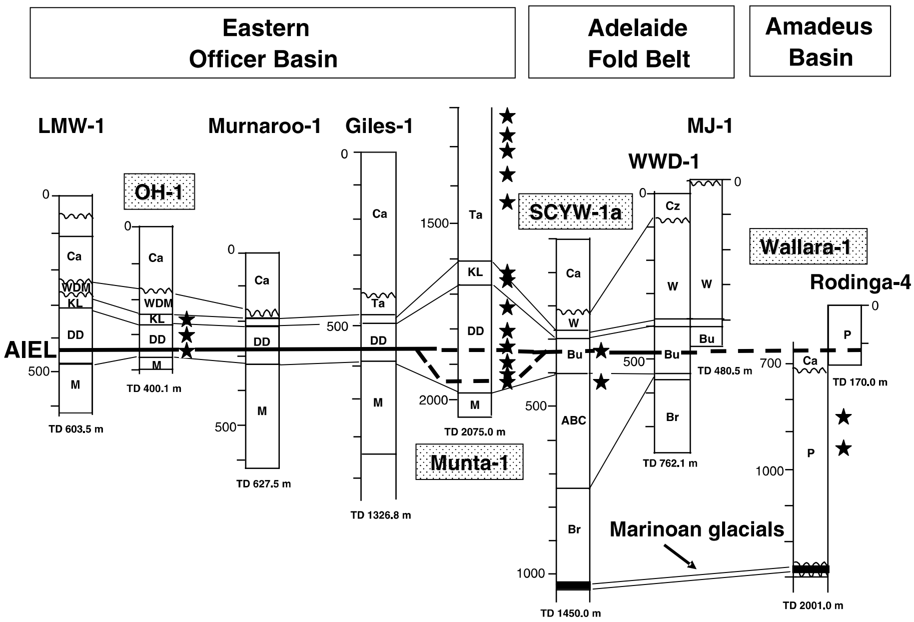

Fig. 2. Stratigraphic correlation showing relationship of drill-hole sections sampled for palynological evaluation (Grey, 1998, 2005; Grey et al., 2003) and organic geochemical analysis (Webster, 2001; Webster et al., 2004; this study). Ta = Tanana Formation; KL = Karlaya Formation; DD = Dey Dey Mudstone; BU = Bunyeroo Formation; ABC = ABC Range Quartzite; P = Pertatataka Formation; AIEL = Acraman impact ejecta level (dashed lines = inferred position); star symbols indicate approximate levels sampled for organic geochemical analysis.

for the most part are unsuitable for biomarker analysis because of their elevated thermal maturity (kerogen H/C = 0.2–0.5; >2% R_o equivalent: McKirdy et al., 2001). However, the thinner condensed Ediacaran section on the adjacent Stuart Shelf is less mature (<1% R_o equivalent: this study) and hence was sampled at the SCYW-1a well locality.

3.2. Screening and extraction

Decimetre lengths of quarter core, cut from the original core (55 mm diameter) with a water-lubricated diamond saw, were selected on the basis of their mudstone lithofacies, dark brown to grey colour and lack of obvious fractures and veins. Thin sections prepared from the core samples that appeared laminated in hand specimen were examined using transmitted white light microscopy and scanning electron microscopy. In preparation for geochemical analysis, the core was scrubbed clean with a wire brush, thoroughly rinsed in water, washed in distilled ethanol and air-dried. The cleaned core was then crushed to chips and pulverised in a solvent-washed Siebtechnik mill. All samples were screened for TOC content at Geotech, Perth, WA. Powdered core (40–150 g) was Soxhlet-extracted with dichloromethane–methanol (93:7 v/v) for 72 h. Solvent was removed by rotary evaporation. The recovered extractable organic matter (EOM) was then fractionated into saturated hydrocarbons, aromatic hydrocarbons and NSO compounds with open-column liquid chromatography using petroleum ether, dichloromethane and methanol as the eluting solvents.

3.3. GC–MS

The saturated and aromatic hydrocarbon fractions were analysed using a Hewlett-Packard 6890 GC interfaced with a mass selective detector (HP MSD 5973). A 30-m capillary column (HP5MS, cross-linked 5% phenylmethylsiloxane, 0.25 mm i.d., 0.25 μm film thickness) was used with helium as the carrier gas. The instrument was operated and the data acquired as described in Othman et al. (2001). The hopane (C_{27}–C_{35} 17αH plus Ts) and regular sterane (C_{27}–C_{29}) distributions were quantified by integration of peak areas in the m/z 191 and m/z 217 chromatograms, respectively. In the latter, C_{27} ααα and αββ 20R steranes were corrected for co-elution of C_{29} 20R and 20S diasteranes via determination of the C_{29}/C_{27} diasterane ratio

Table 2
Stratigraphic location, depositional setting, organic richness, extract yield, thermal maturity and key biomarker parameters of Ediacaran marine sedimentary rocks from four drill holes in the Centralian Superbasin and Adelaide Fold Belt

Drillhole and formation	Depth (m)	Depositional setting[a]	TOC (%)	EOM (ppm)	Rc[b] (%)	Steranes[c]		Ster/Hop[d]	Pr/Ph
						27:28:29	29/27		
Munta-1, Officer Basin									
Tanana[a]	1209.5	Upper slope	0.08	nd	nd	19:30:51	2.7	0.30	1.0
	1216.0		0.09	nd	nd	28:16:56	2.0	0.05	2.2
	1234.0		0.15	nd	nd	36:12:52	1.4	0.05	nd
	1252.2n		0.07	nd	nd	33:16:51	1.5	0.13	0.5
	1252.2m		0.15	nd	nd	31:17:52	1.8	0.08	nd
	1264.8		0.10	nd	nd	36:22:42	1.2	0.10	nd
	1324.8		0.06	nd	nd	25:14:61	2.6	0.04	0.6
	1347.4		0.10	nd	nd	32:20:48	1.5	0.20	nd
	1438.3n	Shelf	0.12	nd	nd	48:12:40	0.8	0.03	1.3
	1438.3m		nd	nd	nd	35:12:53	1.5	0.03	nd
	1443.6n		0.12	nd	nd	10:11:79	8.0	0.02	0.9
	1443.6m		0.30	nd	nd	7:12:81	11.2	0.03	1.4
Karlaya	1648.43m		0.09	114	0.66	17:22:61	3.5	0.06	1.1
	1648.45m		0.15	272	0.67	25:22:53	2.1	0.08	1.1
	1648.47n		0.06	80	0.68	34:25:41	1.2	0.23	0.8
	1648.63m		0.10	95	0.71	28:24:48	1.7	0.13	1.2
	1648.70m		0.08	175	0.70	32:23:45	1.4	0.16	1.2
	1664.82		0.10	137	nd	26:22:52[f]	2.0[f]	0.16	1.3
Dey Dey	1688.62	Upper slope	0.07	90	0.66	32:23:45	1.4	0.09	1.3
	1699.29		0.02	70	nd	38:25:37	1.0	0.32	0.7
	1728.19m		0.21	261	0.68	15:17:68	4.5	0.04	2.0
	1728.19n		0.09	78	nd	18:26:56	3.2	0.06	1.1
	1746.04		0.04	75	nd	40:25:35	0.9	0.30	0.8
	1789.25		0.08	43	nd	34:25:41	1.2	0.30	1.1
	1800.67	Lower slope	0.20[e]	133[e]	nd	21:26:53[e]	2.5[e]	0.11[e]	nd
	1810.55m		1.09	349	0.74	7:18:75	11.4	0.06	1.1
	1810.55n		0.10	77	nd	31:23:46	1.5	0.22	0.7
	1811.05		0.05	24	nd	33:25:42	1.3	0.41	2.0
	1817.86		0.04	35	0.73	30:24:46	1.5	0.34	1.7
	1834.74		0.04	51	nd	34:26:40	1.2	0.37	1.3
	1839.25		0.05	29	nd	40:21:39	1.0	0.42	1.5
	1844.22		0.05	25	nd	31:24:45	1.5	0.37	0.8
	1849.12		0.05[e]	73[e]	nd	33:24:42[e]	1.3[e]	0.25[e]	1.0
	1854.90	Basin floor	0.04	39	nd	35:23:42	1.2	0.42	0.9
	1856.01		0.05	39	0.65	39:22:39	1.0	0.41	0.5
	1856.42		0.06	61	nd	12:21:67	5.6	0.07	0.8
	1856.50	Upper limit of estimated level of Acraman impact ejecta layer[g]							
	1856.59		0.04	50	nd	24:28:48	2.0	0.35	0.9
	1861.22		0.05	40	0.69	32:22:46	1.4	0.29	0.7
	1867.99		0.04	39	nd	26:22:52	2.0	0.26	0.9
	1872.81		0.03	52	nd	31:23:46	1.5	0.33	1.4
	1881.03		0.02	65	0.79	39:24:37	0.95	0.48	1.0
	1884.29		0.05	48	nd	32:24:44[f]	1.4[f]	0.38	0.7
	1890.06		0.04	46	nd	31:22:47	1.5	0.36	1.2
	1895.56		0.06	14	nd	31:23:46	1.5	0.23	0.6
	1899.78		0.05	33	nd	30:23:47	1.6	0.34	0.9
	1914.19		0.07	29	nd	27:22:51	1.9	0.12	1.2
	1923.04		0.05	22	0.76	27:24:49	1.8	0.21	1.4
	1941.92		0.03	40	0.81	27:23:50	1.8	0.20	1.0
	1945.00	Lower limit of estimated level of Acraman impact ejecta layer[g]							
	1952.13		0.02	63	nd	38:24:38	1.0	0.25	0.8
Observatory Hill-1, Officer Basin									
Karlaya	241.70	Shelf	0.06	153	nd	20:14:66	3.4	0.10	1.0

Table 2 (*continued*)

Drillhole and formation	Depth (m)	Depositional setting[a]	TOC (%)	EOM (ppm)	Rc[b] (%)	Steranes[c]		Ster/Hop[d]	Pr/Ph
						27:28:29	29/27		
	243.80		0.07	195	nd	17:14:69	4.0	0.07	0.9
	260.33		0.37	382	nd	11:9:80	6.9	0.03	1.4
	264.12		0.14	165	0.56	28:15:57	2.0	0.03	1.1
Dey Dey	279.37	Upper slope	0.06	193	0.52	35:23:42	1.2	0.19	0.9
	355.00	Acraman impact ejecta layer							
	360.31		0.02	118	nd	41:24:35	0.84	0.26	0.84
SCYW-1a, Adelaide Fold Belt (pre-impact)									
Yarloo[h]	323.30	Outer shelf	0.04	317	nd	42:26:32	0.76	0.35	0.9
ABC Range	400.06	Inner shelf	0.10	231	0.71	41:36:22	0.78	0.45	0.6
	411.46		0.08	321	0.93	37:29:34	0.91	0.46	0.5
Wallara-1, Amadeus Basin (pre-impact)									
Pertatataka	1152	Mid-slope	0.11	130	0.91	33:27:40	1.2	0.37	0.9
	1240		0.25	90	1.35	33:25:42	1.3	0.27	0.8

TOC = total organic carbon; EOM = extractable organic matter; Rc = calculated vitrinite reflectance; Pr/Ph = pristane/phytane; nd = not determined; m = microbial mat, n = non-mat facies at same depth.

[a] Data from Arouri et al. (2000b).

[b] Derived from methylphenanthrene index (MPI-1) using calibration of Radke and Welte (1983).

[c] Regular sterane ratios based on all four isomers of cholestane, 24-methylcholestane and 24-ethylcholestane.

[d] $\sum C_{27}$–C_{29} steranes/$\sum C_{27}$–C_{35} hopanes.

[e] Mean of replicate analyses (Appendix 1).

[f] Mean of quadruplicate GC–MS-SIM analyses of same total alkane fraction (Appendix 2).

[g] Inferred upper limit of AIEL based on palynology, isotope chemostratigraphy and occurrence of fractured crystals (Table 5; Grey, 2005). Inferred lower limit constrained by height of the ejecta layer above the base of the Dey Dey Mudstone in the nearby Giles-1 well (Hill et al., 2004).

[h] Equivalent of Bunyeroo Formation on the Stuart Shelf.

from the m/z 259 chromatogram. For measurement of the methylphenanthrene index (MPI-1: Radke and Welte, 1983), a response factor of 0.69 was employed for phenanthrene.

3.4. Palynological analysis

Samples of the Dey Dey Mudstone ($n = 9$) from an interval in the Munta-1 well, previously regarded as barren of microfossils, were selected for isolation and identification of their palynomorph assemblages. These were processed using the HCl/HF maceration technique of Grey (1999).

4. Results and discussion

The stratigraphic position relative to the Acraman impact level, lithofacies, depositional setting, organic richness, extract yield, thermal maturity and selected biomarker ratios for the 49 rock samples, plus 12 examined by Arouri et al. (2000b), are summarised in Table 2. Similar data from other marine Ediacaran ($n = 10$, all post-impact) and pre-Ediacaran ($n = 3$) sedimentary rocks from the Centralian Superbasin (Summons and Powell, 1991; Logan et al., 1997) are presented in Tables 3 and 4, respectively. Descriptions of acritarchs and their associated dispersed organic matter (Table 5) supplement the palynomorph distributions previously documented by Grey (1998, 2005) and Grey et al. (2003) for the Dey Dey Mudstone at the Munta-1 well. Representative m/z 217 mass fragmentograms, illustrating the stratigraphic variability of Ediacaran sterane distributions, are shown in Fig. 3. The secular variation in the C_{29}/C_{27} sterane ratio and leiosphere versus acanthomorph occurrence is summarised in Fig. 4 and the biomarker response to the Acraman impact is highlighted in Fig. 5.

4.1. Organic richness and thermal maturity

TOC contents of these grey-green to dark brown, fine-grained sediments are typically low (<0.25 wt%). Elevated values (as high as 1.1 wt%) tend to be associated with intervals where benthic

Table 3
Stratigraphic location, organic richness, extract yield, thermal maturity and biomarker parameters of post-impact Ediacaran marine sedimentary rocks from other drill holes in the Centralian Superbasin (after Logan et al., 1997)

Drillhole and formation	Depth (m)	TOC (%)	EOM (ppm)	Rc[a] (%)	Steranes		Pr/Ph
					27:28:29	29/27	
Officer Basin							
Ungoolya-1							
Narana	1320	0.72	156	nd	19:32:49	2.6	0.7
	1322	0.28	125	nd	15:25:60	4.0	0.5
	1393	0.13	35	nd	27:27:46	1.7	1.2
Marla-9							
Tanana	210	0.80	240	0.80	nd	nd	1.0
	256	nd	89	nd	19:15:66	3.5	1.1
	268	0.39	212	0.83	nd	nd	1.0
Karlaya-1							
Dey Dey	2093	0.95	2340	0.79	9:9:82	9.1	1.1
Amadeus Basin							
Rodinga-4A							
Pertatataka	86	0.22	32	nd	29:26:45	1.6	0.7

See Table 2 for key.
[a] Data from McKirdy and Michaelsen (1994).

Table 4
Stratigraphic location, organic richness, extract yield, thermal maturity and biomarker parameters of pre-impact Ediacaran and Cryogenian marine sedimentary rocks from drill holes in the Centralian Superbasin (after Summons and Powell, 1991; Logan et al., 1997)

Drillhole and formation	Depth (m)	TOC (%)	EOM (ppm)	T_{max} (°C)	Steranes		Pr/Ph
					27:28:29	29/27	
Amadeus Basin							
Ooraminna-1							
Pertatataka	625	0.11	182	–	39:27:34	0.87	2.5
	718	0.13	71	–	38:30:32	0.84	0.7
Bluebush-1							
Bitter Springs	2088	0.23	–	–	48:20:32	0.67	2.4
	2089	0.13	164	404	41:23:36	0.88	1.8
Mount Charlotte-1							
Bitter Springs	1654	0.31	2039	430	46:24:30	0.65	1.3

See Table 2 for key.

microbial mats (Logan et al., 1997; Arouri et al., 2000b) are strongly developed. EOM yields likewise are low (Karlaya Limestone, 80–382 ppm; Dey Dey Mudstone, 14–349 ppm; ABC Range Quartzite, 231–321 ppm; Pertatataka Formation, 90–130 ppm: Table 2).

Thermal maturity (MPI-derived Rc values) ranges from 0.5–0.6% in the Karlaya Limestone at the Observatory Hill-1 well, 0.6–0.8% in the Dey Dey Mudstone at the Munta-1 well and 0.7–0.9% in shales of the ABC Range Quartzite at the SCYW-1A drill-hole, to 0.9–1.35% in the Pertatataka Formation at the Wallara-1 well (Table 2). The corresponding TAI values for the Dey Dey are 3− to 4− (Table 5).

The organic leanness of the majority of the samples, together with their considerable antiquity (>540 m.y.), heightens their susceptibility to contamination by non-indigenous hydrocarbons, thereby raising questions as to their suitability for organic geochemical analysis (cf. Peters et al., 2005, pp. 101–102). However, there are strong reasons for believing that the biomarkers reported herein are indigenous to the host rocks and hence reliable indicators of the source affinity of their dispersed organic matter:

Table 5
Summary of palynological analysis of Dey Dey Formation, Munta-1

Sample depth (m)	TAI[a]	Preservation	Comments[b]	Palynoflora[c]	Fractured crystals common
1681.30[d]		Good	*Ab/Am/Vp* acanthomorph assemblage	ECAP	
1687.40[d]		Good	*Ab/Am/Vp* acanthomorph assemblage	ECAP	
1702.90[d]		Good	*Ab/Am/Vp* acanthomorph assemblage	ECAP	
1728.19	3+ to 4−	Poor	Mainly FDOM and LOAF (some may be degraded acanthomorph acritarch fragments), and rare pyrite-coated filaments. Two degraded specimens of ? *Alicesphaeridium medusoidum*. Several specimens with degraded processes or spines may be? *Vidalia pulchra*. One very degraded specimen of ? *Tanarium* sp.	ECAP	Yes
1728.40[d]		Good	*Ab/Am/Vp* acanthomorph assemblage	ECAP	
1736.80[d]		Good	*Ab/Am/Vp* acanthomorph assemblage	ECAP	
1800.90[d]		Good	*Ab/Am/Vp* acanthomorph assemblage	ECAP	
1810.50[d]		Good	*Ab/Am/Vp* acanthomorph assemblage	ECAP	
1810.55	3+	Very poor	FDOM, LOAF, degraded acanthomorphs (<5%), filaments (<1%)	?ECAP	Yes
1821.80[d]		Poor	Degraded acritarchs		
1834.10[d]		Poor	Degraded acritarchs		
1839.25	3−	Poor	FDOM, LOAF, degraded acanthomorphs (<5%) including one specimen with stumps of spines, filaments (<1%)	ECAP	Yes
1845.10[d]			Barren		
1849.12	3+	Poor	FDOM, LOAF, degraded acanthomorphs (<5%) including one specimen of ? *Appendisphaera minutiforma*, together with other very degraded specimens of a similar nature, smaller darker spheres that appear to be degraded leiospheres, rare filaments (<1%)	ECAP	Yes
1852.00[d]		Poor	Degraded acritarchs		
1856.01	3− to 3+	Very poor	FDOM abundant, several degraded spheres, nothing identifiable	?	?
1856.42	3+ to 4−	Very poor	FDOM abundant, several degraded spheres including one large sphere, nothing identifiable	?	Yes
1856.50	Upper limit of estimated level of Acraman impact ejecta layer				
1856.59	3+ to 4−	Very poor	FDOM abundant, several degraded spheres, mostly small and dark, including a few specimens of ? *Leiosphaeridia crassa* and one specimen of ? *Leiosphaeridia jacutica*	?ELP	No
1884.20[d]			Barren		
1895.56	3+	Very poor	FDOM abundant, several degraded spheres, nothing identifiable	?	No
1905.30[d]			Barren		
1923.04	3+ to 4−	Very poor	FDOM abundant, several degraded, pyrite-coated spheres, nothing identifiable	?	No
1926.00[d]			Barren		
1951.50[d]			FDOM	?	
1962.70[d]			Degraded spheroidal acritarchs and filaments together with FDOM, LOAF	?	
1967.20[d]		Good	*Leiosphaeridia crassa*, *Leiosphaeridia minutissima* and degraded spheroidal acritarchs; *Siphonophycus* sp. and degraded filaments together with FDOM, LOAF	ELP	

[a] Thermal alteration index (after Traverse, 1988).
[b] FDOM = finely disseminated organic material; LOAF = large organic amorphous fragments; *Ab/Am/Vp* = *Appendisphaera barbata/Appendisphaera minutiforma/Vidalia pulchra* assemblage (Grey, 1998, 2005).
[c] ECAP = Ediacaran complex acanthomorph palynoflora; ELP = Ediacaran leiosphere palynoflora (Grey et al., 2003; Grey, 2005).
[d] Data from Grey (1998, 2005).

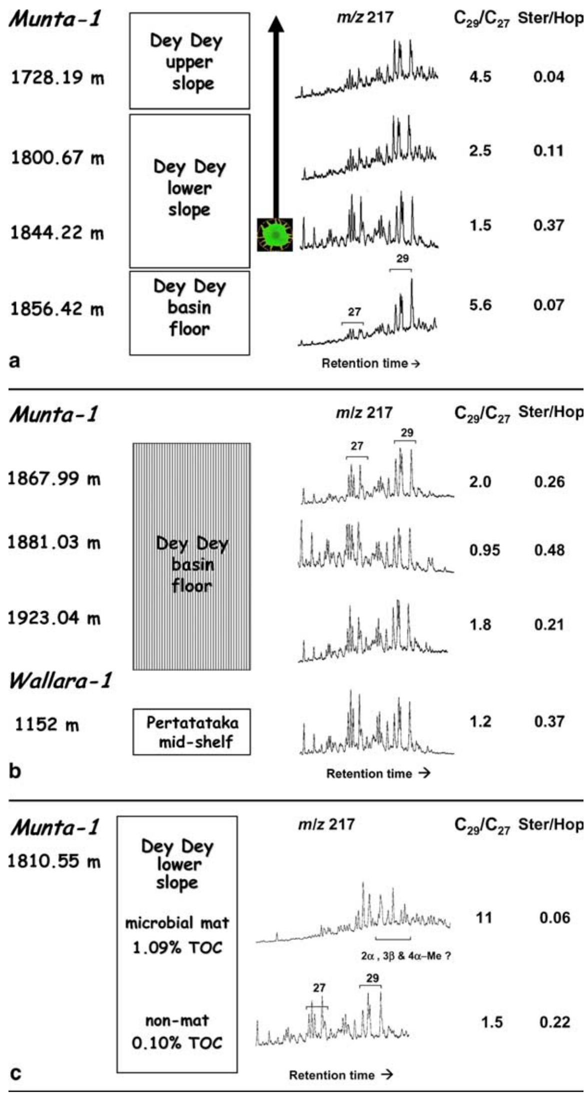

Fig. 3. Representative m/z 217 mass chromatograms and biomarker ratios showing stratigraphic variation of sterane distributions and abundance: (a) post-Acraman impact event (AIE); (b) pre- and immediate post-AIE (vertical shading corresponds to depth interval in Munta-1 well wherein the impact level is most likely to occur); (c) comparison of benthic microbial mat and non-mat sediments from the same depth in the lower slope facies of the Dey Dey Mudstone.

1. All the samples were portions of drill cores recovered from depths well below the weathering profile.
2. Rigorous sample selection, preparation and analytical procedures minimised the risk of adventitious contamination.
3. The low TOC contents and EOM yields are entirely consistent with their deep water depositional settings.
4. Mudstones displaying laminated textures typical of microbial mats are organically richer than adjacent non-laminated lithofacies.
5. There is no evidence of migrated petroleum in the intervals sampled.
6. Replicate analysis of sub-samples of the same homogeneous core length revealed good reproducibility (Appendix 1).
7. Repeat GC–MS analyses of the same alkane fraction demonstrated excellent reproducibility of sterane distributions (Appendix 2).
8. Biomarker and compound-specific isotopic studies of similarly lean rocks from the same Ediacaran depocentres by other workers (Summons and Powell, 1991; Logan et al., 1997, 1999; Arouri et al., 2000b; Hill et al., 2000) yielded comparable, geologically coherent datasets.

4.2. Acritarch preservation and abundance, Munta-1 well

Organic matter in the Dey Dey Mudstone is for the most part very poorly preserved. Of the 26 core samples, only eight yielded acritarchs that could be taxonomically identified with confidence (Table 5). Macerates comprise mainly finely disseminated organic material (FDOM) of uncertain origin and large organic amorphous fragments (LOAFs). In some samples, LOAFs may consist of fragments of degraded acanthomorph acritarchs.

Although some specimens are too poorly preserved to be identified taxonomically, traces of processes (spiny protrusions of the vesicle wall >5% of the vesicle diameter in length) or ornament (protrusions of the vesicle wall <5% of the vesicle diameter), and the size, colour and texture of rare degraded spheres can be used to indicate whether the structure was originally a leiosphere or an acanthomorph. Such degraded specimens have to be treated with extreme caution because they can be confused with amorphous artefacts and only those that showed at least some indication of a vesicle wall were considered. Specimens interpreted as acanthomorphs generally show traces of processes (stumps, ghost-like process shapes), are >75 μm (and usually >100 μm) in diameter and the wall tends to be light orange brown, thin walled and hyaline. By contrast, leiospheres tend to be smaller than 100 μm (and mostly <75 μm), dark brown, thick walled, and scabrate. Previous studies included examination of taphonomic variability (Grey, 1998 and unpublished data), thus enabling

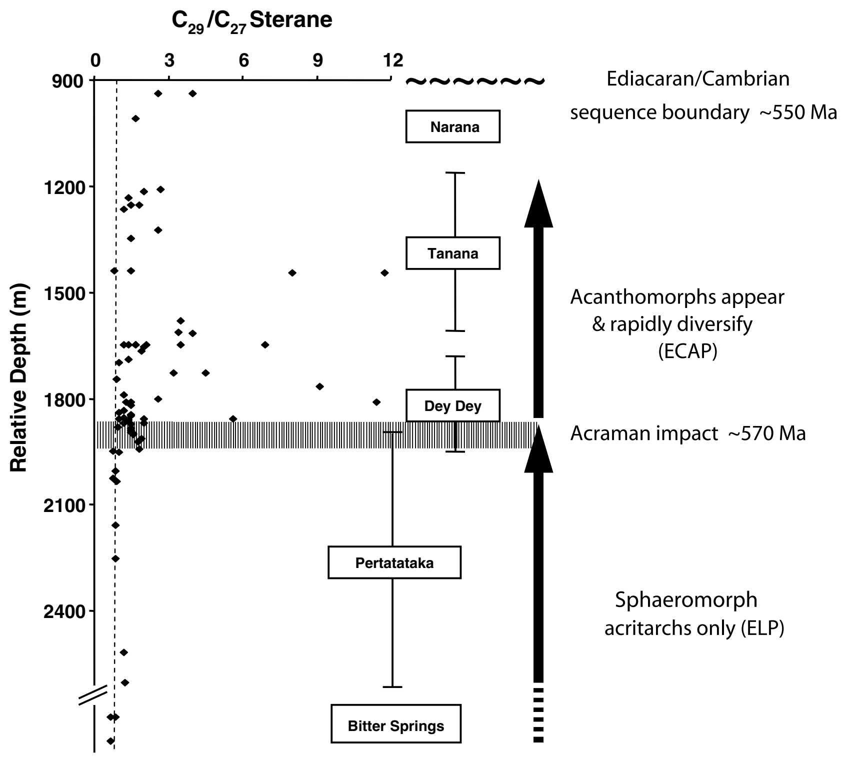

Fig. 4. Composite plot of C_{29}/C_{27} sterane ratio versus stratigraphic depth showing relationship of biomarker variation to lithostratigraphy (host formation), Acraman impact event and acritarch zonation. The Karlaya Limestone (not labelled) lies between the Dey Dey Mudstone and Tanana Formation. Depth scale refers to the Munta-1 well. Samples from other wells plotted relative to their positions above base of host formation. Dashed line corresponds to equal abundance of cholestane and ethylcholestane. Shaded zone defines upper and lower limits of Acraman impact ejecta level in Munta-1 well.

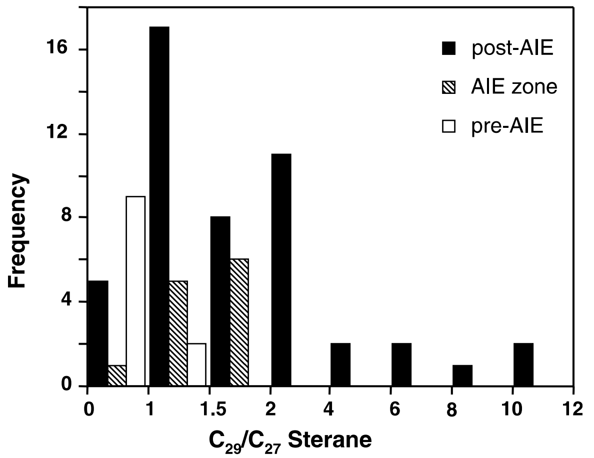

Fig. 5. Frequency distribution of C_{29}/C_{27} sterane values in the following sample categories: (a) pre-AIE, (b) between upper and lower limits of Acraman ejecta level in Munta-1 well and (c) post-AIE.

comparison of severely degraded specimens from the current samples with those observed in earlier samples that show a complete range from well preserved to badly degraded. Hence, it was possible to assign some badly preserved samples to either the Ediacaran complex acanthomorph palynoflora (ECAP) or the Ediacaran leiosphere palynoflora (ELP), thereby narrowing the interval in which the transition occurs from that reported in previous studies.

Small zircons and other acid-insoluble, non-silicate crystals (possibly rutile and carborundum) occur in many of the palynological residues because they were not subjected to heavy liquid separation (Grey, 1999). A large percentage of crystals in the samples above 1856.5 m depth in the Munta-1 well are fractured (Table 4). Some have a mosaic fracture pattern whereas others resemble shock lamellae (primary deformation features: see Fig. 3 in Hill et al., 2004). Preliminary observations suggest that a change from non-fractured crystals to fractured crystals coincides with the first sample that contains probable acanthomorphs. It is possible that this fractured versus non-fractured crystal distribution can be used to indicate the position of the Acraman ejecta layer (Hill et al., 2004).

The available data reveal that acanthomorphs occur from 1849.12 m upward, while leiospheres are present from 1856.59 m downward. The status of samples from 1856.01 and 1856.42 m is unclear, but the presence of a large pale acritarch in core from 1856.42 m suggests these two samples might fall within the ECAP palynoflora. This distribution is consistent with previous results from the Munta-1 well (Grey, 1998, 2005; Grey et al., 2003), and appears to be supported by the presence of shattered crystals in the samples. It is also consistent with the change in sterane distribution and abundance (Tables 2–4) discussed below. Although the poor preservation of the palynomorphs renders any conclusions tentative, the ejecta layer appears to be no higher than 1856.59 m, but could lie as low as 1962.7 m. The latter inference is supported by the position of the AIEL in the nearby Giles-1 well (28.1 m above the base of the Dey Dey Mudstone) and the observed increase in the C_{29}/C_{27} sterane ratio between 1952.13 and 1941.92 m depth in the Munta-1 well (Table 2).

4.3. Biomarker facies

Three main biomarker facies are recognised in the sediments examined (Webster, 2001). All are characterised by the co-occurrence of prominent even-carbon numbered *n*-alkanes (C_{16}–C_{22+}) and pairs of novel highly branched alkanes eluting between *n*-C_{13} and at least *n*-C_{24}. The latter compounds were first identified in samples of the Tanana Formation by Arouri et al. (2000a,b) and subsequently assigned to C_{3n} series E and F by Greenwood et al. (2004). Although no specific source biota are yet known, the latter authors (p. 343) provisionally attribute both of these alkane classes to "bacteria that exploit the redox gradients ... in anoxic and/or euxinic environments and include organisms involved in either the sulfur or nitrogen cycles". Moreover, since these branched alkanes are particularly abundant in deep water sediments of the Dey Dey Mudstone, their likely microbial sources are anaerobic *non-photosynthetic* endobionts, including heterotrophs and chemotrophs. Long-chain *n*-alkanes (C_{23}–C_{37+}, maximum at C_{31}) exhibiting moderate odd-carbon number predominance at C_{27}, C_{29}, C_{31} and C_{33} are common to all three facies and so are probably derived from planktonic photoautotrophs (Logan et al., 1999).

Facies 1 corresponds to the deep basin floor sediments of the Dey Dey Mudstone and the 'non-mat', mid-shelf shales of the Pertatataka Formation. *Facies 2* is developed within muds and silts of the upper Dey Dey Mudstone deposited as turbidites on the lower and upper slope, and in micritic carbonates of the shelfal Karlaya Limestone. It is distinguished from Facies 1 by its lack of even carbon number predominance in the shorter-chain *n*-alkanes and a much lower abundance of series E and F branched alkanes. These two facies have similar hopane (C_{27}–C_{35}) and desmethyl sterane ($C_{29} \geqslant C_{27} > C_{28} > C_{30}$) distributions. Among the homohopanes, C_{35} is commonly more abundant than $C_{34,}$ consistent with pristane/phytane ratios <1, both parameters indicating anoxicity. Microbial mats (assigned to *Facies 3*) occur throughout the same stratigraphic interval as Facies 2. Their pristane/phytane ratios are low (<2) but their *n*-alkane profiles are far from uniform, ranging from unimodal (maximum at C_{16} or C_{31}) to bimodal (maxima at C_{15} and C_{31}) with even and odd carbon number preference expressed to differing extents below and above C_{23}, respectively. Moreover, their sterane/hopane ratios are lower than those in stratigraphically adjacent 'non-mat' sediments. Interestingly, they lack the mid-chain monomethyl and dimethyl alkanes found in the above mentioned microbial mats of the Pertatataka and Tanana Formations and variously considered as markers of sulfide oxidising bacteria or cyanobacteria (Arouri et al., 2000b; Greenwood et al., 2004 and references therein).

4.4. Sterane signatures

Of the benthic and planktonic inputs to these Ediacaran marine sediments, it is the eukaryotic algae and other photoautotrophs that are most likely to provide any biomarker evidence of the environmental havoc wrought by the 'Acraman' impact, an inference supported by the acritarch record (Grey et al., 2003). The C_{29}/C_{27} sterane ratio is largely independent of organic facies and depositional setting and increases from 0.7–1.3 below the ejecta horizon to 1–11 above it (Tables 2–4; Figs. 4 and 5). Samples from the Yarloo Shale and ABC Range Quartzite in the SCYW-1a drill hole (Table 2; Fig. 2) yield C_{29}/C_{27} sterane values <1 (Table 2), thereby constraining the pre-impact chemostratigraphy shown in Fig. 4. Moreover, similar cholestane-dominant sterane signatures have been reported for the lower Pertatataka Formation and the pre-Ediacaran Bitter Springs Formation

($\sim$835 Ma) in the Amadeus Basin (Logan et al., 1999; Hill et al., 2000: see also Table 4). Conversely, markedly elevated relative abundances of ethylcholestane that first appear in the upper Dey Dey Formation also occur higher in the Ediacaran succession of the Officer Basin, notably in the Karlaya Limestone and the Tanana Formation and just below the erosive Neoproterozoic/Cambrian boundary in the upper Narana Formation (Tables 2 and 3). The latter sequence boundary is assigned an age of 550 Ma by Walter et al. (2000).

It may be significant that the highest C_{29}/C_{27} sterane values tend to be recorded in the most organic-rich samples (TOC = 0.30–1.09%). As already mentioned, such intervals are likely to include benthic microbial mats. This raises the possibility that the primary algal steroids in these sediments may have undergone bacterial modification. Elevated abundances of 2α- and 3β-methylsteranes in the Dey Dey Mudstone's benthic mat facies from 1810.55 m in the Munta-1 well (Fig. 3c) indicate that this may indeed have occurred. However, there is no evidence that such early diagenetic microbial alkylation of Δ^2-sterenes (Summons and Capon, 1991; Dahl et al., 1992) favours the C_{27} homologue, thereby decreasing its concentration relative to Δ^2-stigmasterene and resulting in a higher C_{29}/C_{27} sterane ratio. A more feasible explanation for the increased proportion of 24-ethylcholestane among the desmethylsteranes in these richer, microbially laminated sediments is the likely contribution of cyanobacteria to their organic matter. As pointed out by Volkman et al. (1998), "Many cyanobacteria … contain high proportions of 24-ethylcholesterol compared with other sterols, although concentrations per cell are low". The same authors go on to note): "C_{29} sterols having a C-24 ethyl substituent and Δ^7 double bond are also abundant in many green microalgae". Other authors (e.g., Ourisson et al., 1987; Summons et al., 2001) dispute the possibility of de novo synthesis of sterols by cyanobacteria and attribute their reported occurrence in cultures of some species to contamination by yeasts and fungi. According to Volkman (2005), it is still possible that a few extant cyanobacterial species have the ability to synthesise sterols, although their low cellular abundances "make it unlikely that cyanobacteria are a significant source of sterols in sediments". This is certainly the case for sediments of Phanerozoic age. However, it is not necessarily true for Neoproterozoic marine sediments, particularly those deposited beneath an ocean with an impoverished ecosystem depleted by the concerted effects of the most severe ice age in Earth history and a catastrophic asteroid impact (see below).

The ethylcholestane dominated sterane signatures in certain Neoproterozoic sediments and their associated crude oils that pre-date the emergence of vascular plants have been attributed to chlorophyte algae (Summons and Walter, 1990; McKirdy and Imbus, 1992). This signature in Ediacaran marine sediments of the Officer Basin, *deposited soon after the Acraman impact*, casts new light on its origin. The magnitude of the sterane anomaly and its coincidence with the post-Acraman appearance and diversification of acanthomorph acritarchs (Fig. 4; Grey et al., 2003, Fig. 2) suggests that primitive cyst-forming chlorophytes with a robust reproductive cycle survived in the immediate aftermath of the impact, whereas other algae were less resilient (Grey, 1998). The ability to form cysts is a survival strategy, later most notably exploited by dinoflagellates (Brasier, 1980). The anomaly is not evident in every sample analysed from this interval, nor is there a steady increase in C_{29}/C_{27} sterane ratio between the AIEL and the apparent acme of ethylcholestane dominance around 1443 m depth in the Munta-1 well (Fig. 4). This may simply reflect transient spikes in primary productivity as the acanthomorphs started to develop and diversify. The anomaly persists, albeit perhaps sporadically, from the AIEL to within 37 m of the regional unconformity that is the upper boundary of the Ediacaran sequence in the Ungoolya-1 well.

A fourfold drop in sterane/hopane ratios corresponds to a negative shift of 4‰ in $\delta\ ^{13}$C org at about this time (Calver and Lindsay, 1998), both consistent with a sharp decline in marine algal productivity following the Acraman impact (as discussed above). The biomarker signature of this global catastrophe, based on the timescale of Walter et al. (2000), has an estimated duration of $\sim$20 million years. Moreover, the depleted ranks of the phytoplankton, and their diminished productivity, make it more likely that the primary chlorophyte ethylcholestane-dominant signature would be enhanced in intervals that include benthic cyanobacterial mats. This may well account for the high C_{29}/C_{27} sterane values (8–11) recorded in mat-bearing core samples from the carbonate shelf lithofacies of the younger Tanana Formation at 1443.6 m depth in the Munta-1 well (Table 2, Fig. 4).

4.5. Chemical and taxonomic affinities of Ediacaran acanthomorph microfossils

A phyletic link between chlorophytes and acanthomorphs is suggested by the trilaminar sheath (TLS)-bearing wall structure and highly aliphatic *n*-alkylpolymethylenic composition of two spinose acritarchs from the Karlaya Limestone and Tanana Formation (Fig. 2: Arouri et al., 1999). Both features are characterisitc of algaenan-bearing chlorophytes. However, in a follow up study of four additional acanthomorph species from the Tanana and Pertatataka Formations (Fig. 2), Arouri et al. (2000a) found that their cell walls were of several types. Each wall type has fine laminations, but without obvious TLS and comprises "a polyaromatic biomacromolecule of high recalcitrance". The latter feature suggests "a possible link between acanthomorph taxa and dinoflagellates" (Arouri et al., 2000a). On the other hand, upon undertaking ultrastructural and biomarker analysis of *Tanarium conoideum* (one of the same acanthomorphs examined by Arouri et al., 2000a), Javaux et al. (2004) concluded that this spiny acritarch "contains a biopolymer consisting of long chained polymethylenic material similar to algaenan isolated from some green micro-algae".

Many acritarch species have been assigned to the class Prasinophyceae (Colbath and Grenfell, 1995). However, prasinophyte characteristics are not evident in most Ediacaran species and their affinities remain unclear (Grey, 2005). Likewise, despite their remarkable similarity to certain dinoflagellate taxa, Ediacaran acritarchs cannot be included in the Dinophyceae because they lack an archaeopyle and other features diagnostic of post-Permian dinocysts. Talyzina and Moczydlowska (2000) examined the wall ultrastructure of several acritarch species from the Cambrian Lükati Formation of Estonia. They concluded that *Tasmanites* and some species of *Leiosphaeridia* have pore canals consistent with a prasinophyte origin, but other taxa are more likely to be chlorophycean algae. Surprisingly, another specimen of *Leiosphaeridia* exhibits a composite and multi-layered wall ultrastructure quite unlike the simple, non-laminar structure reported for the Ediacaran leiosphere examined by Arouri et al. (2000a) but reminiscent of that in extant Chlorophyceae. Thus, what was previously regarded as a morphologically simple 'genus' turns out to have diverse biological affinities.

While further studies are obviously needed to elaborate and clarify the chemotaxonomy of Ediacaran organic walled microfossils, sufficient data are available to support the conclusion that large acanthomorph species belong to a short-lived group of rapidly diversifying, probably chlorophycean algae. Their emergence may well have provided a food source for the Ediacaran metazoan fauna, which ultimately brought about their demise through over grazing (Grey, 2005).

4.6. Implications for Neoproterozoic petroleum systems

Crude oils with anomalous desmethylsterane signatures ($C_{29}/C_{27} = 4$–22) occur in Russia (Bazhenova and Arefiev, 1997) and Oman (the Huqf oil family: Grantham et al., 1988). Interestingly, the published data for both of these oil groups suggest that their inferred Neoproterozoic source rocks are somewhat less enriched in ethylcholestane ($C_{29}/C_{27} = 1.2$–3.8). Similar signatures have been reported for Siberian oils (Fowler and Douglas, 1987; Summons and Powell, 1992) and characterise the Dey Dey petroleum system in the eastern Officer Basin, South Australia (Tingate and McKirdy, 2003). Heavy, sulfur-rich oil produced from the 'Infracambrian' Jodhpur Formation in the Baghewala-1 well in northwestern India also has a high C_{29}/C_{27} sterane ratio (3.0), like another heavy crude from the 'Infracambrian' Salt Range Series in the nearby Karampur-1 well in Pakistan (5.1: Peters et al., 1995). The widespread occurrence of these atypical signatures in late Neoproterozoic basins that were located close to the palaeoequator (Li and Powell, 2001) prompts the question: do they reflect the response of the global marine biosphere to the Acraman impact?

Currently, the South Oman Salt Basin is the only one of the depocentres in question where sufficient biomarker, geochronological and stable carbon isotope chemostratigraphic data are available to address this question. Here, three end-member Huqf oil types correlate with the pre-salt Shuram and Buah Formations, the intra-salt 'U' Shale and the intra-salt Athel Silicilyte, respectively (Terken et al., 2001). All the oil types are C_{29} sterane-dominant and isotopically very "light" (whole-oil $\delta^{13}C = -35$ to $-40‰$). Comparison of the carbon isotopic profiles of the Omani (Burns and Matter, 1993; Amthor et al., 2003) and Australian (Calver and Lindsay, 1998; Grey et al., 2003) successions

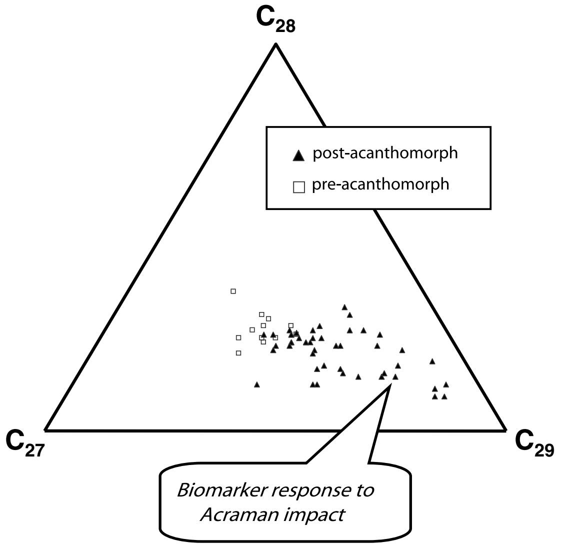

Fig. 6. Sterane ternary plot highlighting the biomarker response to the AIE.

reveals that the Shuram and Buah source rocks and their oils are likely to contain biomarker and isotopic evidence of the post-Acraman biotic crisis. This conclusion rests heavily on the assumed time equivalence of the negative δ^{13}C excursions at the base of the Shuram (~10‰) and low in the Dey Dey (~4‰. If these two formations do indeed encode isotopic and molecular 'fingerprints' of the Acraman asteroid impact and resulting biotic crisis, then it is significant that its effects, especially the sterane anomaly, appear to have persisted into the Early Cambrian, as evidenced by the intra-salt 'U' and Athel source rocks of the Omani succession.

Further work is required to evaluate the possibility that the markedly ethylcholestane-dominant signatures of certain Neoproterozoic and Cambrian source rocks and crude oils from Oman, Pakistan, India, Russia, Siberia and Australia all may be markers of the Acraman impact (Fig. 6).

5. Conclusions

Sterane biomarker data from the Ediacaran (Late Neoproterozoic) sediments of Central Australia are consistent with stable carbon isotopic and palynofloral evidence indicating the catastrophic effect of the Acraman asteroid impact on life in the 'post-Snowball' global ocean. Amplification of the C_{29}/C_{27} sterane ratio was delayed (by ~0.5 million year) but thereafter was prolonged (estimated duration at least 20 million years). This primary signal may reflect the enhanced survival of certain chlorophyte algae, possibly due to their encysting lifestyle.

The highest C_{29}/C_{27} sterane values typically occur in the most organic-rich sediments (along with higher relative concentrations of 2α and 3β-methylsteranes), suggesting bacterial modification of primary algal steroids during early diagenesis. However, this is unlikely to have altered the proportions of the preserved desmethylsteranes in favour of the C_{29} homologue. On the other hand, cyanobacteria may have preferentially contributed 24-ethylcholesterol in some microbial mats from shallower marine settings (e.g., carbonate shelf), thereby augmenting the input from planktonic chlorophytes.

The most likely potential source rocks for Huqf-type crude oils in the eastern Officer Basin are the upper slope Dey Dey Mudstone and the shelfal Karlaya Limestone. The characteristic ethylcholestane-dominant sterane distribution of all three Huqf oil families in Oman can tentatively be linked to the post-Acraman biotic crisis.

Acknowledgements

An earlier version of this paper was presented at the 21st International Meeting on Organic Geochemistry, Krakow, in September 2003. D.Mc.K. and L.W. wish to thank the Petroleum Branch of the Department of Primary Industries and Resources, South Australia, for financial support and for allowing them access to drill cores from the Officer Basin and Stuart Shelf. Dr Jamie Burgess (then with the Northern Territory Geological Survey) kindly provided the core samples from the Wallara-1 well. L.W. acknowledges support from an Australian Postgraduate Award and an AAPG Grant-in-Aid. K.G. publishes with the permission of the Director, Geological Survey of Western Australia. Some of her work for this study was carried out while in receipt of an Australian Postgraduate Award at Macquarie University, and in later stages, in part, as an associate researcher with the Australian Centre for Astrobiology, Macquarie University and the School of Earth Science, Monash University. Finally, the authors are grateful to George Williams, Peter Boult, Kenneth Peters and Jochen Brocks for their helpful reviews of the manuscript and to Andreas Schmidt-Mumm for his assistance with computer drafting.

Appendix 1. Repeat analyses of contiguous core samples from two intervals of Dey Dey Mudstone, Munta-1

Depth (m)		TOC (%)	Weight (g)	EOM (ppm)	Steranes		Ster/Hop
					27:28:29	29/27	
1800.67–1800.80		0.20	130	59	21:27:52	2.5	0.10
		0.20	21	207	21:25:54	2.6	0.11
	Mean:	0.20		133	21:26:53	2.5	0.11
1849.12–1849.24		0.053	40	60[a]	34:23:43	1.3	0.22
		0.048	91	104	37:25:38	1.0	0.32
		0.050	75	55	30:24:46	1.5	0.21
	Mean:	0.050		73	33:24:42	1.3	0.25

See Table 2 for key.
[a] Sustained minor loss of sample during evaporation of solvent.

Appendix 2. Repeat GC–MS–SIM analyses of steranes in total alkane fractions of two core extracts, Munta-1

Depth (m)	Formation		TOC (%)	EOM (ppm)	Steranes	
					27:28:29	29/27
1664.82	Karlaya		0.10	137	25:20:54	2.2
					26:26:48	1.8
					28:21:51	1.8
					26:20:54	2.0
		Mean:			26:22:52	2.0
1884.29	Dey Dey		0.050	48	36:23:41	1.1
					33:24:43	1.3
					30:23:47	1.6
					30:26:44	1.5
		Mean:			32:24:44	1.4

See Table 2 for key.

Associate Editor—**K.E. Peters**

References

Amthor, J.E., Grotzinger, J.P., Schröder, S., Bowring, S.A., Ramezani, J., Martin, M.W., Matter, A., 2003. Extinction of *Cloudina* and *Namacalathus* at the Precambrian-Cambrian boundary in Oman. Geology 31, 431–434.

Arouri, K., Greenwood, P.F., Walter, M.R., 1999. A possible chlorophycean affinity of some Neoproterozoic acritarchs. Organic Geochemistry 30, 1323–1337.

Arouri, K.R., Greenwood, P.F., Walter, M.R., 2000a. Biological affinities of Neoproterozoic acritarchs from Australia: microscopic and chemical characterisation. Organic Geochemistry 31, 75–89.

Arouri, K., Conaghan, P.J., Walter, M.R., Bischoff, G.C.O., Grey, K., 2000b. Reconnaissance sedimentology and hydrocarbon biomarkers of Ediacarian microbial mats and acritarchs, lower Ungoolya Group, Officer Basin. Precambrian Research 100, 235–280.

Bazhenova, O.K., Arefiev, O.A., 1997. Geochemical peculiarities of Pre-Cambrian source rocks in the East European Platform. Organic Geochemistry 25, 341–351.

Becker, L., Poreda, R.J., Bunch, T.E., 2000. Fullerenes: an extraterrestrial carbon carrier phase for noble gases. Proceedings of the National Academy of Science USA 97, 2979–2983.

Becker, L., Poreda, R.J., Hunt, A.G., Bunch, T.E., Rampino, M., 2001. Impact event at the Permian-Triassic boundary: evidence from extraterrestrial noble gases in fullerenes. Science 291, 1530–1533.

Bowring, S., Myrow, P., Landing, E., Ramezani, J., Grotzinger, J., 2003. Geochronological constraints on terminal Neoproterozoic events and the rise of metazoans. Geophysical Research Abstracts 5, 13219.

Brasier, M.D., 1980. Microfossils. Chapman & Hall, London, 193 pp.

Burns, S.J., Matter, A., 1993. Carbon isotope record of the latest Proterozoic from Oman. Eclogae Geologicae Helvetiae 86, 595–607.

Calver, C.R., 1998. Isotope stratigraphy of the Neoproterozoic Togari Group, Tasmania. Australian Journal of Earth Sciences 45, 865–874.

Calver, C.R., 2000. Isotope stratigraphy of the Ediacarian (Neoproterozoic III) of the Adelaide Rift Complex, South Australia, and the overprint of water column stratification. Precambrian Research 100, 121–150.

Calver, C.R., Lindsay, J.F., 1998. Ediacarian sequence and isotope stratigraphy of the Officer Basin, South Australia. Australian Journal of Earth Sciences 45, 513–532.

Calver, C.R., Walter, M.R., 2000. The late Neoproterozoic Grassy Group of King Island, Tasmania: correlation and palaeogeographic significance. Precambrian Research 100, 299–312.

Calver, C.R., Black, L.P., Everard, J.L., Seymour, D.B., 2004. U–Pb zircon age constraints on late Neoproterozoic glaciation in Tasmania. Geology 32, 893–896.

Coccioni, R., Basso, D., Brinkhuis, H., Galeotti, S., Gardin, S., Monechi, S., Spezzaferri, S., 2000. Marine biotic signals across a late Eocene impact layer at Massignano, Italy: evidence for long-term environmental perturbations?. Terra Nova 12 258–263.

Colbath, G.K., Grenfell, H.R., 1995. Review of biological affinities of Paleozoic acid-resistant, organic-walled eukaryotic algal microfossils (including 'acritarchs'). Review of Palaeobotany and Palynology 86, 287–314.

Dahl, J., Moldowan, J.M., McCaffrey, M.A., Lipton, P.A., 1992. 3-Alkyl steranes in petroleum: evidence for a new class of natural products. Nature 355, 154–157.

Foster, C.B., Logan, G.A., Summons, R.E., Gorter, J.D., Edwards, D.S., 1997. Carbon isotopes, kerogen types and the Permian-Triassic boundary in Australia: implications for exploration. APPEA Journal 37, 472–489.

Fowler, M.G., Douglas, A.G., 1987. Saturated hydrocarbon biomarkers in oils of Late Precambrian age from Eastern Siberia. Organic Geochemistry 11, 201–213.

Gostin, V.A., Haines, P.W., Jenkins, R.J.F., Compston, W., Williams, I.S., 1986. Impact ejecta horizon within late Precambrian shales, Adelaide Geosyncline, South Australia. Science 233, 198–200.

Gostin, V.A., Keays, R.R., Wallace, M.W., 1989. Iridium anomaly from the Acraman impact ejecta horizon: impacts can produce sedimentary iridium peaks. Nature 340, 542–544.

Grantham, P.J., Lijmbach, G.W.M., Posthuma, J., Hughes Clarke, M.W., Willink, R.J., 1988. Origin of crude oils in Oman. Journal of Petroleum Geology 11, 61–80.

Greenwood, P.F., Arouri, K., Logan, G.A., Summons, R.E., 2004. Abundance and geochemical significance of C_{2n} dialkylalkanes and highly branched C_{3n} alkanes in diverse Meso- and Neoproterozoic sediments. Organic Geochemistry 35, 331–346.

Grey, K., 1998. Ediacarian acritarch palynology of Australia. Ph.D. Thesis, Macquarie University, New South Wales, 669 p.

Grey, K., 1999. A modified palynological preparation for the extraction of large Neoproterozoic acanthomorph acritarchs and other acid-insoluble microfossils. Geological Survey of Western Australia, Record 1999/10, 23 pp.

Grey, K., 2001. Surviving the Snowball Earth: the acritarch record. Geological Society of Australia Abstracts 65, 45–47.

Grey, K., 2005. Ediacaran Palynology of Australia. Memoirs of the Australasian Association of Palaeontologists 31, 439 pp.

Grey, K., Walter, M.R., Calver, C.R., 2003. Neoproterozoic biotic diversification: snowball Earth or aftermath of the Acraman impact? Geology 31, 459–462.

Grice, K., Cao, C., Love, G.D., Böttcher, M.E., Twitchett, R.J., Grosjean, E., Summons, R.E., Turgeon, S.C., Dunning, W., Jin, Y., 2005. Photic zone euxinia during the Permian-Triassic superanoxic event. Science 307, 706–709.

Halverson, G.P., Hoffman, P.F., Schrag, D.P., Maloof, A.C., Rice, A.H.N., 2005. Toward a Neoproterozoic composite carbon-isotope record. GSA Bulletin 117, 1181–1207.

Heymann, D., Chibante, L.P.F., Brooks, R.R., Wolbach, W.S., Smalley, R.S., 1994. Fullerenes in the Cretaceous-Tertiary boundary layer. Science 265, 645–647.

Hill, A.C., Arouri, K., Gorjan, P., Walter, M.R., 2000. Geochemistry of marine and nonmarine environments of a Neoproterozoic cratonic carbonate/evaporite: the Bitter Springs Formation, Central Australia. In: Grotzinger, J.P., James, N.P. (Eds.), Carbonate Sedimentation and Diagenesis in the Evolving Precambrian World. SEPM Special Publication 67, pp. 327–344.

Hill, A.C., Grey, K., Gostin, V.A., Webster, L.J., 2004. New records of the Late Neoproterozoic Acraman ejecta in the Officer Basin. Australian Journal of Earth Sciences 51, 47–51.

Hoffmann, K.-H., Condon, D.J., Bowring, S.A., Crowley, J.L., 2004. U-Pb zircon date from the Neoproterozoic Ghaub Formation, Namibia: Constraints on Marinoan glaciation. Geology 32, 817–820.

Holser, W.T., 1997. Geochemical events documented in inorganic carbon isotopes. Palaeogeography, Palaeoclimatology, Palaeoecology 132, 173–182.

Hsü, K.J., McKenzie, J.A., 1990. Carbon-isotope anomalies at era boundaries; global catastrophes and their ultimate cause. In: Sharpton, V.L., Ward, P.D. (Eds.), Global Catastrophes in Earth History: An Interdisciplinary Conference on Impacts, Volcanism and Mass Mortality, Boulder, CO. Geological Society of America Special Paper 247, pp. 61–70.

Ivaney, L.D., Salawitch, R.J., 1993. Carbon isotopic evidence for biomass burning at the K-T boundary. Geology 21, 487–490.

Javaux, E.J., Marshall, C.P., Knoll, A.H., Walter, M.R., 2004. Protistan evolution in the Precambrian: a new multidisciplinary approach combining microscopy and microchemistry. Geological Society of America, Abstracts with Programs 36, 399.

Jenkins, R.J.F., Reid, P., Nedin, C., Jansyn, J., 1998. Meteorite impact horizon and lonestones in Bunyeroo Formation. In: Jenkins, R.J.F., McKirdy, D.M., Nedin, C. (Compilers), The Ediacaran in South Australia: Proposal and Field Guide Supporting GSSP Position 'C' at Wearing Dolomite, Flinders Ranges, 16–22 June 1998. IUGS Working Group on the Terminal Proterozoic System, pp. 44–45.

Knoll, A.H., Walter, M.R., Narbonne, G.M., Christie-Blick, N., 2004. A new period for the geological time scale. Science 305, 621–622.

Kring, D.A., 2000. Impact events and their effect on the origin, evolution and distribution of life. GSA Today 10, 1–7.

Li, Z.X., Powell, C.M., 2001. An outline of the paleogeographic evolution of the Australasian region since the beginning of the Neoproterozoic. Earth-Science Reviews 53, 237–277.

Logan, G.A., Summons, R.E., Hayes, J.M., 1997. An isotopic biogeochemical study of Neoproterozoic and Early Cambrian sediments from the Centralian Superbasin, Australia. Geochimica et Cosmochimica Acta 61, 5391–5409.

Logan, G.A., Calver, C.R., Gorjan, P., Summons, R.E., Hayes, J.M., Walter, M.R., 1999. Terminal Proterozoic mid-shelf benthic microbial mats in the Centralian Superbasin and their environmental significance. Geochimica et Cosmochimica Acta 63, 1345–1358.

Margaritz, M., 1989. ^{13}C minima follow extinction events: a clue to faunal radiation. Geology 17, 337–340.

Martin, D., Grazhdankin, D.V., Bowring, S.A., Evans, D.A.D., Fedonkin, M.A., Kirschvink, J.L., 1999. Age of Neoproterozoic bilaterian body and trace fossils, White Sea, Russia: implications for metazoan evolution. Science 288, 841–845.

McKirdy, D.M., Imbus, S.W., 1992. Precambrian petroleum: a decade of changing perceptions. In: Schidlowski, M., Golubic, S., Kimberley, M.M., McKirdy, D.M., Trudinger, P.A. (Eds.), Early Organic Evolution: Implications for Mineral and Energy Resources. Springer, Berlin, pp. 176–192.

McKirdy, D.M., Michaelsen, B.H., 1994. Geochemical measurements of thermal maturity in Neoproterozoic and Cambrian sediments, eastern Officer Basin. Report for South Australian Department of Mines and Energy, Open file Envelope 8488, pp. 65–96 (unpublished).

McKirdy, D.M., Burgess, J.M., Lemon, N.M., Yu, X., Cooper, A.M., Gostin, V.A., Jenkins, R.J.F., Both, R.A., 2001. A chemostratigraphic overview of the late Cryogenian interglacial sequence in the Adelaide Fold-Thrust Belt, South Australia. Precambrian Research 106, 149–186.

McLaren, D.J., Goodfellow, W.D., 1990. Geological and biological consequences of giant impacts. Annual Review of Earth and Planetary Sciences 18, 121–171.

Othman, R., Arouri, K.R., Ward, C.R., McKirdy, D.M., 2001. Oil generation by igneous intrusions in the northern Gunnedah Basin, Australia. Organic Geochemistry 32, 1219–1232.

Ourisson, G., Rohmer, M., Poralla, K., 1987. Prokaryotic hopanoids and other polyterpenoid sterol surrogates. Annual Reviews of Microbiology 41, 301–333.

Peters, K.E., Walters, C.C., Moldowan, J.M., 2005. The Biomarker Guide: Biomarkers and Isotopes in the Environment and Human History, second ed. Cambridge University Press, Cambridge, pp. 101–102.

Peters, K.E., Clark, M.E., Das Gupta, U., McCaffrey, M.A., Lee, C.Y., 1995. Recognition of an Infracambrian source rock based on biomarkers in the Baghewala-1 oil, India. AAPG Bulletin 79, 1481–1494.

Poag, C.W., 1997. Roadblocks on the kill curve: testing the Raup hypothesis. Palaios 12, 582–590.

Preiss, W.V., 2000. The Adelaide Geosyncline of South Australia and its significance in Neoproterozoic continental reconstruction. Precambrian Research 100, 21–63.

Radke, M., Welte, D.H., 1983. The methylphenanthrene index (MPI): a maturity parameter based on aromatic hydrocarbons. In: Bjoroy, M. et al. (Eds.), Advances in Organic Geochemistry 1981. Wiley, Chichester, pp. 504–512.

Raup, D.M., 1992. Large-body impact and extinction in the Phanerozoic. Paleobiology 18, 80–88.

Summons, R.E., Walter, M.R., 1990. Molecular fossils and microfossils of prokaryotes and protists from Proterozoic sediments. American Journal of Science A 290, 212–244.

Summons, R.E., Capon, R.J., 1991. Identification and significance of 3β-ethyl steranes in sediments and petroleum. Geochimica et Cosmochimica Acta 55, 2391–2395.

Summons, R.E., Powell, T.G., 1991. Petroleum source rocks of the Amadeus Basin. In: Korsch, R.J., Kennard, J.M. (Eds.), The Amadeus Basin, Bulletin 236. Bureau of Mineral Resources, Canberra, pp. 511–524.

Summons, R.E., Powell, T.G., 1992. Hydrocarbon composition of Late Proterozoic oils of the Siberian Platform: implications for the depositional environment of source rocks. In: Schidlowski, M., Golubic, S., Kimberley, M.M., McKirdy, D.M., Trudinger, P.A. (Eds.), Early Organic Evolution: Implications for Mineral and Energy Resources. Springer, Berlin, pp. 296–307.

Summons, R.E., Jahnke, L., Cullings, K.W., Logan, G.A., 2001. Cyanobacterial biomarkers: triterpenoids plus steroids? EOS, Transactions of the American Geophysical Union 82 (47), Fall Meeting Supplement, Abstract B22D-0184.

Talyzina, N.M., Moczydlowska, M., 2000. Morphological and ultrastructural studies of some acritarchs from the Lower Cambrian Lükati Formation, Estonia. Review of Palaeobotany and Palynology 112, 1–21.

Terken, J.M.J., Frewin, N.L., Indrelid, S.L., 2001. Petroleum systems of Oman: charge timing and risks. AAPG Bulletin 85, 1817–1845.

Tingate, P.R., McKirdy, D.M., 2003. Exploration opportunities in the Officer Basin. South Australian Department of Primary Industries and Resources, Report Book 2003/1, 11 pp.

Toon, O.B., Zahnle, K., Morrison, D., Turco, R.P., Covey, C., 1997. Environmental perturbations caused by the impacts of asteroids and comets. Reviews of Geophysics 35, 41–78.

Traverse, A., 1988. Paleopalynology. Unwin Hyman, Boston, 600 pp.

Venkatesan, M.I., Dahl, J., 1989. Further geochemical evidence for global fires at the Cretaceous-Tertiary boundary. Nature 338, 57–60.

Vlierboom, F.W., Collini, B., Zumberge, J.E., 1986. The occurrence of petroleum in sedimentary rocks of the meteor impact crater at Lake Siljan, Sweden. Organic Geochemistry 10, 153–161.

Volkman, J.K., 2005. Sterols and other triterpenoids: source specificity and evolution of biosynthetic pathways. Organic Geochemistry 36, 139–159.

Volkman, J.K., Barrett, S.M., Blackburn, S.I., Mansour, M.P., Sikes, E.L., Gelin, F., 1998. Microalgal biomarkers: a review of recent research developments. Organic Geochemistry 29, 1163–1179.

Wallace, M.W., Gostin, V.A., Keays, R.R., 1989. Discovery of the Acraman impact ejecta blanket in the Officer Basin and its stratigraphic significance. Australian Journal of Earth Sciences 36, 585–587.

Wallace, M.W., Gostin, V.A., Keays, R.R., 1996. Sedimentology of the Neoproterozoic Acraman impact-ejecta horizon, South Australia. AGSO Journal of Australian Geology and Geophysics 16, 443–451.

Walter, M.R., Veevers, J.J., Calver, C.R., Gorjan, P., Hill, A.C., 2000. Dating the 840–544 Ma Neoproterozoic interval by isotopes of strontium, carbon, and sulfur in seawater, and some interpretative models. Precambrian Research 100, 371–433.

Webster, L., 2001. Terminal Proterozoic biomarker assemblages in the Centralian Superbasin before and after the Acraman meteorite impact. B.Sc. Honours Thesis, University of Adelaide (unpublished).

Webster, L., McKirdy, D., Grey, K., Arouri, K., Gostin, V., 2004. Biomarker and sedimentological signals of concerted environmental stress on the late Neoproterozoic Palaeo-Pacific Ocean. Geological Society of Australia Abstracts 73, 246.

Williams, G.E., 1986. The Acraman impact structure: source of ejecta in late Precambrian shales, South Australia. Science 233, 200–203.

Williams, G.E., 1994. Acraman: a major impact structure from the Neoproterozoic of Australia. In: Dressler, B.O., Grieve, R.A.F., Sharpton, V.L. (Eds.), Large Meteorite Impacts and Planetary Evolution. Geological Society of America, Special Paper 293, pp. 209–224.

Williams, G.E., Wallace, M.W., 2003. The Acraman asteroid impact, South Australia: magnitude and implications for the late Vendian environment. Journal of the Geological Society, London 160, 545–554.

Williams, G., Gostin, V., Wallace, M., 2004. The Acraman impact event, South Australia: recognition, magnitude and implications for the Late Vendian environment. Geological Society of Australia Abstracts 73, 247.

Wolbach, W.S, Gilmour, I., Anders, E., 1990. Major wildfires at the Cretaceous/Tertiary boundary. In: Sharpton, V.L., Ward, P.D. (Eds.), Global Catastrophes in Earth History: An Interdisciplinary Conference on Impacts, Volcanism and Mass Mortality, Boulder, CO. Geological Society of America Special Paper 247, pp. 391–400.

Zhou, C., Tucker, R., Xiao, S., Peng, Z., Yuan, X., Chen, Z., 2004. New constraints on the ages of Neoproterozoic glaciations in south China. Geology 32, 437–440.